ACS APPLIED MATERIALS & INTERFACES

Research Article

www.acsami.org

Cyclodextrin-Functionalized Chromatographic Materials Tailored for Reversible Adsorption

Jessica H. Ennist,‡ Eric A. Gobrogge,‡ Kristian H. Schlick, Robert A. Walker,* and Mary J. Cloninger*

Department of Chemistry and Biochemistry, Montana State University, Bozeman, Montana 59717, United States

Supporting Information

ABSTRACT: Novel dendronized silica substrates were synthesized. First- and second- generation polyaryl ether dendrons were appended to silica surfaces. Using Cu(I) mediated cycloaddition "click" chemistry, β-cyclodextrin was tethered to the dendronized surfaces and to a nondendronized surface for comparison purposes. This synthesis strategy affords a modular, versatile method for surface functionalization in which the density of functional groups can be readily varied by changing the generation of dendron used. The surfaces, which are capable of adsorbing target analytes, have been characterized and studied using X-ray photoelectron spectroscopy (XPS) and vibrational sum frequency spectroscopy (VSFS). Fluorescence spectroscopy was used to study the surfaces' ability to retain coumarin 152 (C152). These studies indicated that the β-cyclodextrin functionalized surfaces not only adsorbed C152 but also retained it through multiple aqueous washes. Furthermore, these observations were quantified and show that substrates functionalized with first-generation dendrons have a more than 6 times greater capacity to adsorb C152 than slides functionalized with monomeric β-cyclodextrin. The first-generation dendrons also have 2 times greater the capacity than the larger generation dendrons. This result is explained by describing a dendron that has an increased number of β-cyclodextrin monomers but, when covalently bound to silica, has a footprint too large to optimize the number of accessible monomers. Overall, both dendronized surfaces demonstrated an increased capacity to adsorb targeted analytes over the slides functionalized with monomeric β-cyclodextrin. The studies reported provide a methodology for characterizing and evaluating the properties of novel, highly functional surfaces.

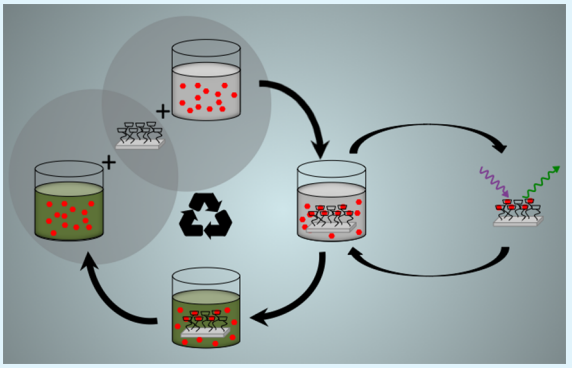

KEYWORDS: *reversible adsorption, dendrimers, dendrons, β-cyclodextrin, silica, XPS, fluorescence, coumarin, SFG*

INTRODUCTION

Removing organic analytes from an aqueous solution plays a critical role in a host of environmental and technology-related challenges. For example, the U.S. Environmental Protection Agency's Safe Drinking Water Act ensures the quality of drinking water by limiting the amounts of over 90 different contaminants, and new contaminants are added to the list every five years.[1] Nearly 60% of these contaminants are organic and have been determined to cause side effects ranging from organ damage to an increased risk of cancer when exposure to the maximum allowed levels are exceeded.[1] Examples include aromatic species used to manufacture insecticides such as benzene (0.005 mg/L) and chlorobenzene (0.1 mg/L), two chemicals that are also used in textile processing. One current and popular method for removing such contaminants from water includes using a high-surface-area substrate such as activated charcoal or soda ash.[2,3] While this method can remove a wide variety of pollutants, the resulting contaminated material cannot be reused and must be disposed of after the sorption process. In applications where large volumes of solution must be processed to remove relatively small amounts of a targeted solute, one ideally wants to employ a system that concentrates the solute and can be recycled for further use.

A recyclable substrate that can remove solutes from solution requires that adsorption be reversible. For reversible adsorption to be a viable mechanism for removing solutes from solution, binding energies must be large enough so that adsorption is thermodynamically favorable under application-specific conditions but weak enough so that solutes will desorb with modest changes in solution phase, temperature, pH, or composition. Such requirements preclude standard covalent bond formation between the substrate and solute and, instead, must rely on reversible interactions to remove organic solutes from aqueous solution.[4] Spontaneous self-assembly and molecular recognition are two common phenomena that rely on noncovalent forces to drive association and aggregation in solution and at surfaces, and from the perspective of reversibly binding solutes to surfaces,[5−7] exploiting the ability of β-cyclodextrin as a host for hydrophobic organic guests is an attractive option.

Surfaces functionalized with β-cyclodextrin have been used to form guest−host inclusion complexes.[8−10] β-Cyclodextrin

Received: July 28, 2014
Accepted: September 24, 2014
Published: September 24, 2014

forms a hydrophobic cavity through a series of α-1,4 linkages between seven glucoside monomers.[11] This structure forms a complex of intramolecular hydrogen bonds, rendering the interior cavity hydrophobic and the exterior surface hydrophilic.[12] Representative binding energies for β-cyclodextrin complexes with organic analytes generally range from −25 to −5 kJ/mol.[8] To put these binding energies into the context of reversible adsorption, equilibrium conditions necessitate that removal of 50% of the solute molecules from a 10 μM aqueous solution at room temperature requires an adsorption (or binding) energy of approximately −19 kJ/mol, and removal of 90% requires an adsorption energy of −24 kJ/mol. In order for the functionalized surface saturated with the bound analyte to be recycled and reused, the analyte desorption must overcome this host−guest association in a way that leaves the surface intact and ready for reuse.

Previous studies have used surface-tethered β-cyclodextrin to form guest−host complexes for numerous purposes such as reversible chlorophenol and chlorobenzene removal[9] and controlled fragrance release.[10] Such surfaces, however, have a capacity limited by the surface coverage of β-cyclodextrin sites. In principle, more sites would improve the substrate's capacity. Work described below overcomes the saturation limitation commonly associated with using functionalized surfaces to promote chemical processes. Surfaces have a limited number of sites that are available to accommodate the adsorption of solutes from solution. By functionalizing silica substrates with dendrimers containing multiple β-cyclodextrin units, we show how the useful ability of β-cyclodextrin to form host−guest self-assemblies can be amplified by the multivalent properties of dendrimer chemistry. Substrates functionalized with first- and second-generation dendrons, as well as surfaces functionalized with only single β-cyclodextrin monomers (Figure 1), are tested for reversible adsorption behavior using Coumarin 152 (C152), a fluorescent organic dye having a trifluoromethyl group in the 4 position and a dimethyl amino group in the 7 position. C152 was chosen for the fluorescence studies because of this solute's well-characterized photophysical behavior in a wide variety of solvents.[13−16] From previous studies, C152's emission wavelength has been shown to shift with solvent polarity due to differences between the ground-state and excited-state dipole moments and the solute's sensitivity to hydrogen bonding opportunities presented by the solvent.[14,16−21] Affinity of the coumarin solutes for the surfaces can be estimated from bulk solution binding constants. The studies reported here demonstrate that C152 has an affinity for the β-cyclodextrin functionalized surfaces and is retained even after multiple washings with a pure aqueous solvent. A small-volume rinse of the saturated surface with methanol results in complete release of the solute. Quantifying these results show that substrates functionalized with first-generation dendrons (containing multiple β-cyclodextrin sites) have a greater capacity than slides functionalized either with monomeric β-cyclodextrin or with higher-order dendrons. This result can be understood in terms of the trade-off between maximizing the number of accessible β-cyclodextrin monomers per dendron versus the number of dendrons that can be covalently bound to a silica substrate.

EXPERIMENTAL METHODS

Materials and Methods. The quartz slides (25 × 25 × 0.5 mm) used in these studies were purchased from SPI Supplies. Prior to experimental use, the quartz slides were cleaned in a 1:1 (v/v) mixture of nitric acid and sulfuric acid (Macron Chemicals) for 1 h and rinsed with deionized water (Millipore, 18.2 MΩ). *N*, *N*′-Dicyclohexylcarbodiimide and all high-purity organic solvents were purchased from Fisher Scientific. All other chemicals used were purchased from Sigma-Aldrich.

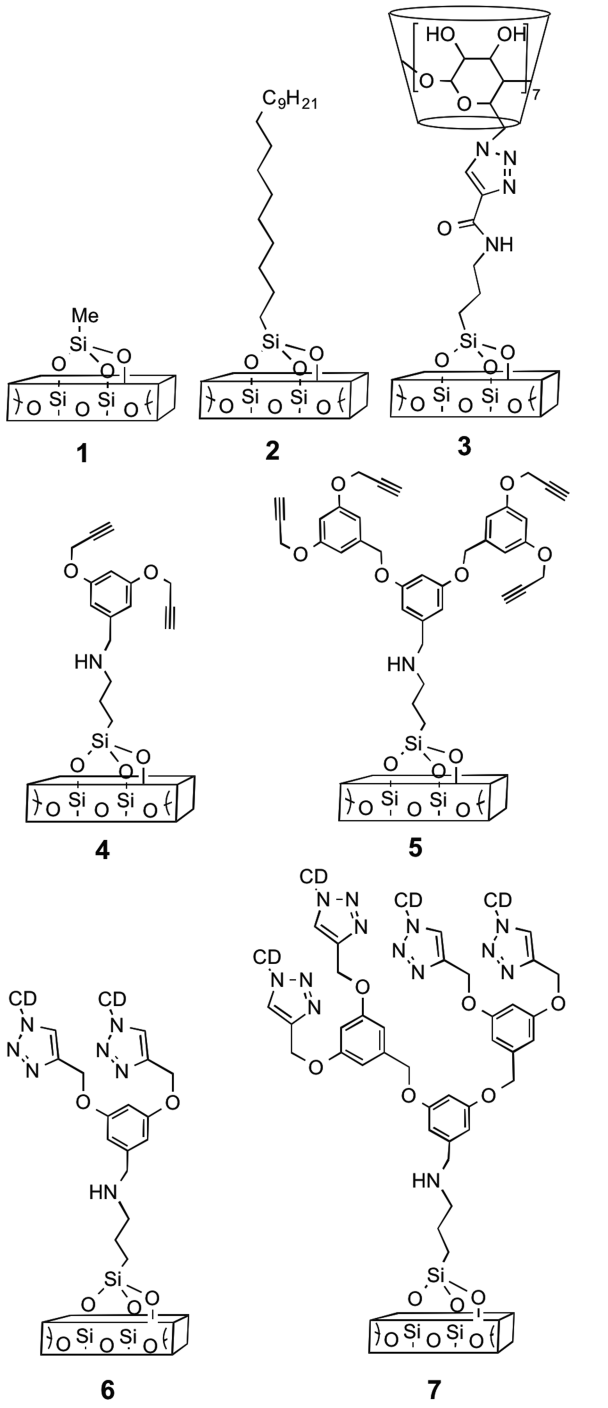

Figure 1. Schematic representations of functionalized surfaces. CD = β-cyclodextrin.

Alkyl Monolayer Functionalized Surfaces 1 and 2. Strategies for creating silica surfaces having different functional group composition were adapted from Jones' SAM formation using THF/Cyclohexane.[22] A 10 mL Teflon beaker equipped with a stir bar was placed inside a 50 mL Teflon beaker. Both beakers were placed inside a sealable glass container with an inert atmosphere. The silica slides were placed along the inside wall of the outer Teflon beaker, and toluene (40 mL) was added. A stock solution of alkyltrichlorosilane

(0.03 mmol in 2 mL of Tetrahydrofuran (THF) and 75 μL of 6 M HCl) was stirred for 4 h at room temperature and added to the 50 mL Teflon beaker. The reaction was allowed to stir for 3 h under argon. To remove excess solvents, slides were sonicated for 3 min in 50 mL of toluene, for 3 min in 50 mL of Milli-Q water (18.2 MΩ·cm), and for 3 min in 50 mL of methanol. The sequential sonications with water and methanol were repeated two more times. Slides were dried under a stream of argon and stored under vacuum.

1-β-Cyclodextrin-*N*-(3-(silyl)propyl)-1,2,3-triazole-4-carboxamide Functionalized Surface 3. Mono-6-deoxy-6-azido-β-cyclodextrin was synthesized using previously described methods.[23,24] *N*-(3-(trimethoxysilyl)propyl)propiolamide was synthesized by the method that was reported for the analogous triethoxy compound.[25] The synthesis of functionalized surface **3** was adapted from silica beads to slides.[26] A 10 mL Teflon beaker equipped with a stir bar was placed inside a 50 mL Teflon beaker. Toluene (40 mL) was added to the 50 mL Teflon beaker, and two slides were placed along the inside wall of the 50 mL Teflon beaker. *N*-(3-(trimethoxysilyl)propyl)propiolamide (90 mg, 390 μmol) was dissolved in the toluene, and the solution was stirred at reflux for 2 h. The slides were washed in 40 mL of toluene. The slides and 40 mL of *N*,*N*-dimethylformamide (DMF) were added to a new 50 mL Teflon beaker equipped with a 10 mL Teflon beaker holding a stir bar and heated to 80 °C. Mono-6-deoxy-6-azido-β-cyclodextrin (330 mg, 280 μmol, 1 equiv) and $CuI(PPh_3)_3$ catalyst (13 mg, 28 μmol, 0.1 equiv) was added, and the reaction was stirred for 4 days. Slides were washed with 40 mL of DMF, and were sonicated for 3 min in 50 mL of toluene. Slides were then sonicated for 3 min in 50 mL of Milli-Q water (18.2 MΩ·cm) and for 3 min in 50 mL of methanol. The sequential sonications with water and methanol were repeated two more times. Slides were dried under a stream of argon and stored under vacuum.

Polyaryl Ether Dendron Functionalized Surfaces 4 and 5. Two generations of polybenzyl ether dendrons were synthesized by previously described methods.[27−29] Silica surfaces were functionalized by general silanization methods.[30,31] The slides were placed along the inside wall of a 50 mL Teflon beaker containing a 10 mL Teflon beaker equipped with a stir bar. 3-Aminopropyltrimethoxysilane was added to 40 mL of toluene in the 50 mL Teflon beaker and refluxed for 2 h. Slides were washed with 40 mL of toluene and were added to a new 50 mL Teflon beaker equipped with a 10 mL Teflon beaker containing a stir bar and 40 mL of toluene. The toluene was brought to reflux, and the dendron (50 μmol) and 2 mL of Hunig's base were added. The reaction was stirred for 2 days. Slides were sonicated for 3 min in 50 mL of toluene. Slides were then sonicated for 3 min in 50 mL of Milli-Q water (18.2 MΩ·cm) and for 3 min in 50 mL of methanol. The sequential sonications with water and methanol were repeated two more times. Slides were dried under a stream of argon and stored under vacuum.

β-Cyclodextrin Functionalized Polyaryl Ether Dendronized Surfaces 6 and 7. Polyaryl ether dendron functionalized slide **4** or **5** was placed along the inside wall of a 50 mL Teflon beaker equipped with a 10 mL Teflon beaker holding a stir bar. DMF (40 mL) was added, and the system was heated to 80 °C. Mono-6-deoxy-6-azido-β-cyclodextrin (110 mg, 100 μmol, 1 equiv) and $CuI(PPh_3)_3$ catalyst (10 μmol, 0.10 equiv) were added and allowed to stir for 2 d. Slides were washed with 40 mL of DMF, and ultrasonically cleaned for 3 min in 50 mL of toluene. Slides were sonicated for 3 min in 50 mL of toluene. Slides were then sonicated for 3 min in 50 mL of Milli-Q water (18.2 MΩ·cm) and for 3 min in 50 mL of methanol. The sequential sonications with water and methanol were repeated two more times. Slides were dried under a stream of argon and stored under vacuum.

X-ray Photoelectron Spectroscopy (XPS). The functionalized slides were characterized using XPS. The analysis was conducted on a Physical Electronics 5600ci XPS system equipped with monochromatized Al Kα X-rays. The analysis area of the sample was 0.8 mm in diameter. Electron emissions were collected at 45° with respect to normal, and the spherical-sector-analyzer pass energy was selected as 23.5 eV for high-resolution scanning and as 46.95 eV for a survey to achieve optimum energy resolution and count rate. Initial representative survey scans were acquired from 0 to 600 eV for 10 sweeps (sw) at 0.4 eV/step, and 20 mS/step (Figure 2). For further elemental analysis, high-resolution scans were acquired for the C 1s

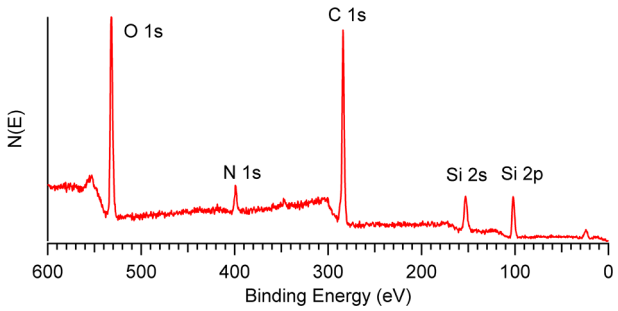

Figure 2. Survey scan of functionalized surface **3**.

(~280 to 291 eV, 2 sw), N 1s (~394 to 405 eV, 5 sw), O 1s (~528 to 537 eV, 2 sw), and Si 2p (~98 to 106 eV, 3 sw) regions. The acquisition parameters were run for 10 cycles at 0.50 eV/step and 20 mS/step. For all spectra, the background of all regions were subtracted using the Shirley background.[32] Peak positions were normalized to the C 1s peak at 285.0 eV and were fitted to functions having a 100% Gaussian line shape. Binding energies were normalized to the C 1s. Data acquisition and data analysis were performed using RBD AugerScan software. Quantitative analysis to determine the site composition was performed using methodologies previously described by Geiger and co-workers.[6] Specific expressions relevant to our analysis are shown in the Supporting Information.

Fluorescence Spectroscopy. The functionalized slides were characterized using fluorescence spectroscopy and the fluorescent dye C152. This system (functionalized surface/fluorescent dye) was used to test the ability of different slides to retain adsorbed analytes. Steady-state fluorescence spectra were recorded using a Jobin Yvon Horiba Fluorolog 3 FL3−11. Bulk measurements were acquired with 1 nm instrumental resolution accumulating signal for 0.5 s at each step. Bulk solution measurements were made with no polarizers in either the excitation or emission paths. Surface fluorescence measurements were acquired in 0.5 nm increments integrating for 1.5 s at each point with the excitation and emission polarizers set 90° apart.[15] This procedure reduced the amount of background scatter in the surface excitation and emission spectra so that adsorbed species could be observed clearly.

To evaluate the ability of β-cyclodextrin-functionalized surfaces to adsorb organic solutes from solution, we characterized the bulk solution behavior of C152 in hexane and aqueous solvents (in the absence and presence of codissolved β-cyclodextrin). All bulk solution experiments were performed with C152 concentrations of 10 μM (2.6 mg/L). To measure the guest−host complex's fluorescence properties, excess (2.3:1 mol ratio) β-cyclodextrin was added to the aqueous solution. For the surface measurements, 10 μM aqueous solutions of C152 were prepared, and functionalized slides were then allowed to equilibrate in the solution for 1 h. Additional equilibration time did not lead to any observed changes in the data. The slides were removed slowly from the solution, and excess solvent was allowed to evaporate from the bottom of the slide. Fluorescence measurements were acquired from the top of the slide, the incident light striking the sample at a 30° angle with respect to normal. Previous studies have shown that this procedure probes adsorbed films that are not influenced by excess solute accumulation following evaporation.[15,33,34] After the initial scan, the slide was immersed in pure Milli-Q water for 60 s and then removed. Excess water was allowed to evaporate, and a second surface fluorescence spectrum was measured. This rinse-and-measure procedure was repeated to test the retention abilities of the functionalized surfaces. Control experiments were performed using the same procedure with unfunctionalized slides and slides that had been functionalized with terminal alkyl monolayers. The hydrophilic control slides were cleaned prior to use by soaking in a 50:50 mixture of concentrated sulfuric and nitric acid. The hydrophobic control slides

were rinsed with excess methanol and dried at ambient temperature before use.

To quantify the amount of analyte bound to the functionalized surfaces, a similar fluorescence procedure was used. The slide of interest was initially allowed to soak again in a 10 μM aqueous solution of C152. After 1 h had elapsed, the slide was removed from the solution, and the excess solvent was allowed to evaporate. Upon evaporation of the solvent, the slide was soaked in water for 60 s, removed, and again allowed to dry. The slide was then washed and sonicated in 50 mL of methanol, and the fluorescence excitation of the wash at C152's emission wavelength (513 nm) was measured. Comparing the excitation intensity of the wash to standard solutions with known concentrations enabled us to quantitatively determine the number of molecules adsorbed to the surface to be determined quantitatively. Assuming a uniform distribution of adsorbates on the surface, these results were converted into surface coverages.

Vibrational Sum Frequency Generation (VSFG). VSFG is a second-order nonlinear optical process that measures vibrational spectra of molecules in environments lacking inversion symmetry. In a VSFG experiment, two high-intensity fields (one visible and one infrared) induce a coherent, nonlinear polarization in molecules at a surface or interface. This polarization oscillates at a frequency equal to the sum of the incident visible and IR fields and is responsible for the detected signal. When the IR frequency is resonant with a vibrational mode of a surface molecule, the sum frequency (SF) response experiences resonance enhancement. By altering the polarization of the light incident on the sample and the polarization at which the SF beam is collected, orientation data from detected surface species can also be obtained by solving for the four independent nonzero elements of the 27 element second order susceptibility tensor. The individual polarizations in such a VSFG experiment are identified by a three-letter symbol (e.g., *ssp* or *sps*) where *s* indicates the electric field vector of the light is parallel to the surface, and *p* indicates the electric field vector is perpendicular to the surface. These three letters represent the polarization of the three frequencies in order of decreasing energy (i.e., SF, visible, IR).[35] A more in-depth description of the SFG process and SFG theory has appeared elsewhere.[35−37]

VSFG characterization employs an assembly described previously.[38] Briefly, the system uses a Libra-HE Ti:sapphire laser (Coherent, 3.3W 85 fs pulse duration, 1 kHz repetition rate) coupled to a visible optical parametric amplifier (Coherent OPerA Solo) to generate IR light. VSFG experiments were performed with copropagating IR and visible fields with both fields passing through the 0.5 mm silica slide and the signal being detected in the reflected direction. The IR wavelength was tuned from 3.2 to 3.7 μm in 0.5 μm increments, and the IR field was focused onto the sample at an angle of 73° with respect to normal. The visible beam was spectrally stretched and sliced using an 1800 g/mm grating and variable width slits resulting in a spectrally narrowed visible beam (20 cm^{-1}). After passing through two different delay stages, this beam was focused onto the surface at an angle of 67° with respect to normal. When the IR and visible fields were spatially and temporally overlapped, sum frequency signal was generated and directed into a monochromator (SpectraPro-300i, Acton Research Corporation) where it was dispersed onto a 1340 × 100 pixel CCD (PIXIS100B, Princeton Instruments). SFG spectra were combined and normalized to a nonresonant gold system response using homemade routines written in Igor Pro (version 6). VSFG spectra were corrected first for IR power using the nonresonant SFG response across the frequency region of interest from a gold-coated silicon wafer. Spectra were then normalized by the SFG signal from a clean, hydrophilic silica/vapor interface acquired under the appropriate polarization condition. All spectra were then calibrated using the 2910 cm^{-1} methyl symmetric stretch of DMSO at the liquid/vapor interface.[39]

A sample VSFG spectrum is shown in Figure 3. This representative figure, taken in the *ssp* polarization combination, shows the C−H stretching region of the solid/vapor interface of a methyl terminated silica surface.

In this sample spectrum, two peaks are evident at 2910 and 2967 cm^{-1}. These two peaks result from the methyl group symmetric and antisymmetric stretch, respectively, and are consistent with previously reported data.[40] The intensity difference between the peaks also suggests that the methyl groups are arranged predominantly with their methyl C_3 axes normal to the surface.

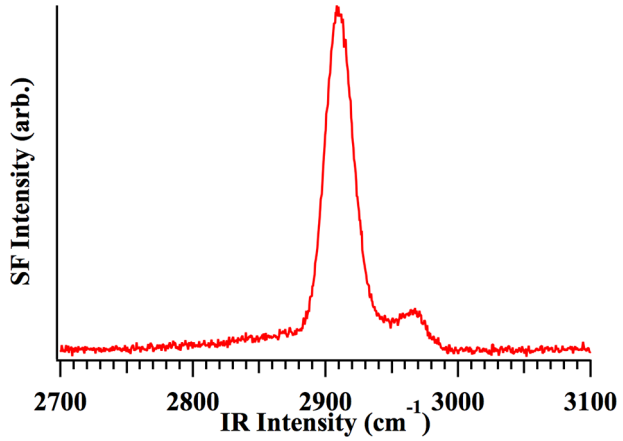

Figure 3. VSFG spectrum of the solid/vapor interface of a methyl-terminated silica substrate in the *ssp* polarization combination.

RESULTS AND DISCUSSION

Silica surfaces were modified to display terminal alkynes by silanization using *N*-(3-(trimethoxysilyl)propyl)propiolamide (**8**). The terminal alkynes **9** were reacted with β-cyclodextrin azide **10** by a Cu(I) mediated cycloaddition[41,42] to afford surface **3** (Scheme 1a). Silica surfaces were modified to display terminal amines by silanization using 3-aminopropyltrimethoxysilane (**11**) to form surface **12**. Addition of the dendron **13** was accomplished by S_N2 displacement of the core bromide by the terminal amines presented on the silica surface to afford surface **4**. The alkyne end groups on the G1 dendron were further modified by a Cu(I) mediated cycloaddition using β-cyclodextrin azide **10** to yield surface **6**.

Prior to characterization, slides were sonicated once in toluene and then three times sequentially in Milli-Q water and methanol. This purification method minimized the environmental carbon and nitrogen that were present on the product slides, as evidenced by XPS. High-resolution narrow scans of the C 1s and N 1s regions of the control after being washed by this purification method are shown in Figure 4. The carbon 1s signal contains contributions from multiple carbon sources. First, the signal was fit with a central peak at 285 eV that was attributed to the binding energy of sp^2 and sp^3 hybridized carbons that are bound to carbon or hydrogens as shown in Figure 4a (C−H/C−C peak). Second, a higher energy peak was fit that was attributed to the oxygen and nitrogen bound sp^3 C 1s emission (C−O/C−N peak in Figure 4a). A third peak was fit that is in agreement with silicon-bound C 1s emission (Si−C peak in Figure 4a).[43,44] The signal from the scan of the N 1s region shown in Figure 4b was minimal (as expected) and is consistent with emission from a small amount of residual nitrogen at the surface.

Surfaces **1** and **2** were fully characterized to assist in the identification of more complicated features of the other surfaces discussed in this work. Figure 5 shows the narrow C 1s spectra of the methyl and octadecyl terminated surfaces. Both of these C 1s signals were fitted with two peaks, the C−H/C−C peak at 285 eV assigned to sp^3 hybridized carbon emission, and the C−Si peak at 283.9 eV assigned to the silicon bound carbon 1s emission.[43] The increased atomic concentration on the surface of **2** was observed in an increased C−H/C−C peak because **2** is

Scheme 1. Synthesis of Functionalized Silica Surfaces

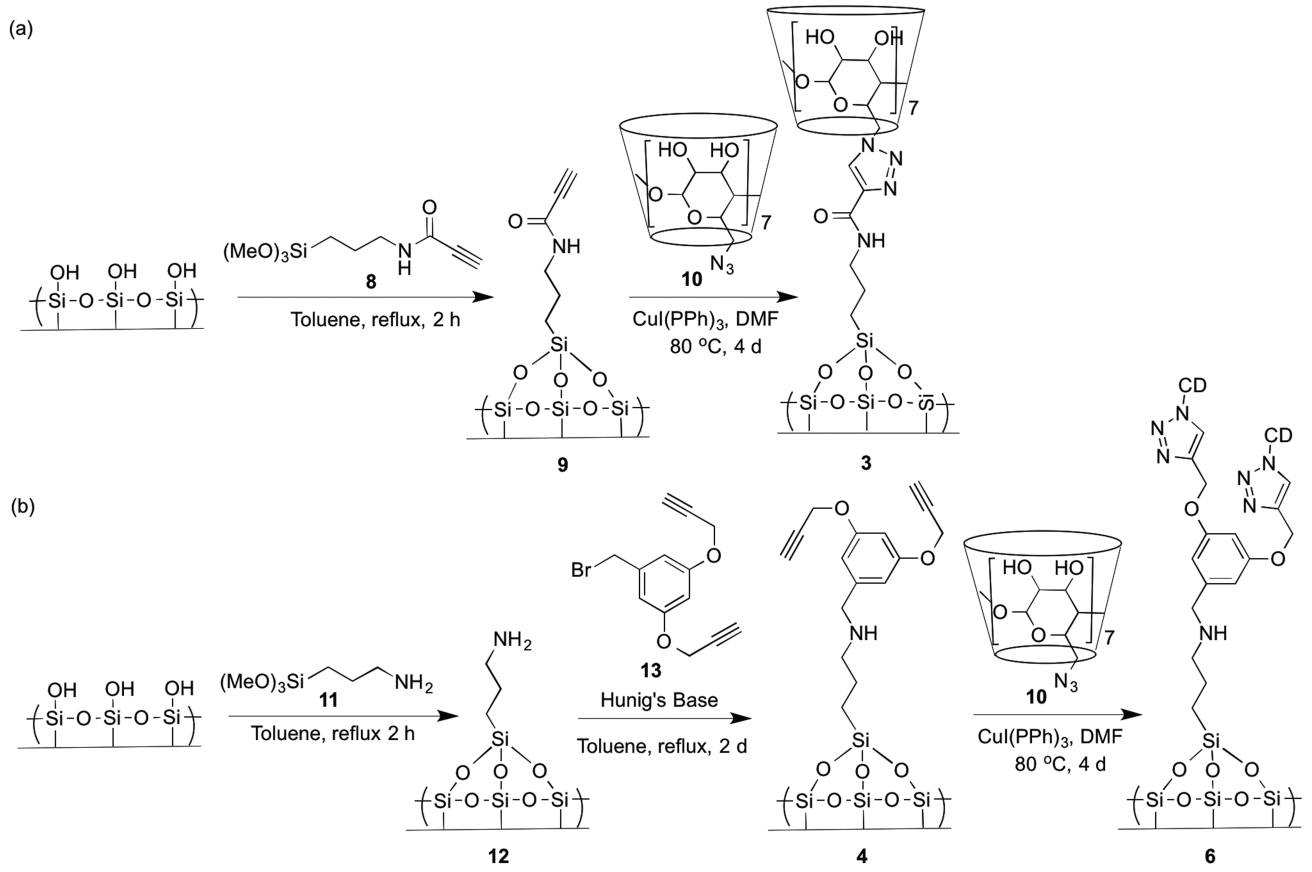

[a] β-Cyclodextrin attachment to the silica surface. [b] Dendronization of the silica surface followed by attachment of β-cyclodextrin to the dendrons.

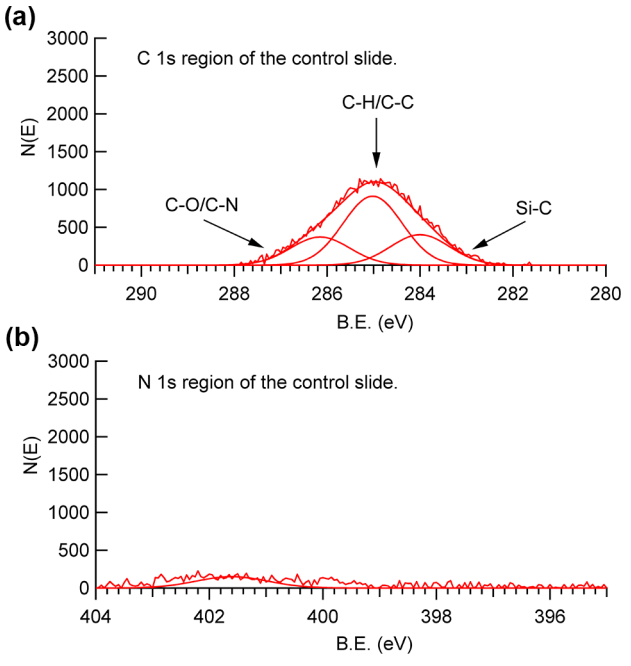

Figure 4. XPS spectra of unfunctionalized surfaces. High-resolution scans of (a) the carbon 1s region and (b) the nitrogen 1s region.

functionalized with an 18 carbon alkyl chain while **1** is functionalized with a single methyl group.

Figure 6 shows the C 1s and N 1s spectra of the 1-β-cyclodextrin-*N*-(3-(silyl)propyl)-1,2,3-triazole-4-carboxamide functionalized surface **3**. In Figure 6a, the C 1s signal was broad with a shoulder centered at 288 eV. The spectrum was deconvoluted into five overlapping peaks in agreement with the expected atomic structure of the organic monolayer. Two peaks, labeled C−H/C−C and C−Si, are consistent with the C 1s emission attributed to sp^3 and sp^2 hybridized carbons and to C−Si bonds, as previously described. The higher energy broadening of the signal was resolved into two peaks. The C═O peak in Figure 6a was fitted under the shoulder and centered at 288 eV. This peak fitting is consistent with both the C 1s emission of the amide carbonyl carbon of the tether and with the anomeric carbons in the β-cyclodextrin. The second peak, which is centered at 286.2 eV, was assigned to the C 1s emission from nitrogen-bound carbons and hydroxyl-bound carbons in the β-cyclodextrin and is labeled C−O/C−N in Figure 6a.[43,45] The lower energy broadening of the signal was fitted with a peak centered at 283.1 eV, in agreement with the emission from the sp hybridized carbons. The sp C peak indicates that some alkynes remain unfunctionalized in the conversion of **9** to **3** (Scheme 1).[46]

Additional evidence of the triazole formation is supported by the higher energy broadening in the N 1s spectrum from surface **3** (Figure 6b), an effect that is absent in data acquired with surface **9** (Figure S1, Supporting Information). This high-energy region is fitted with an additional peak centered at 401.5 eV in agreement with the binding energy of the 1s emission of the central nitrogen (N═N−N) of the triazole.[47,48] Addition-

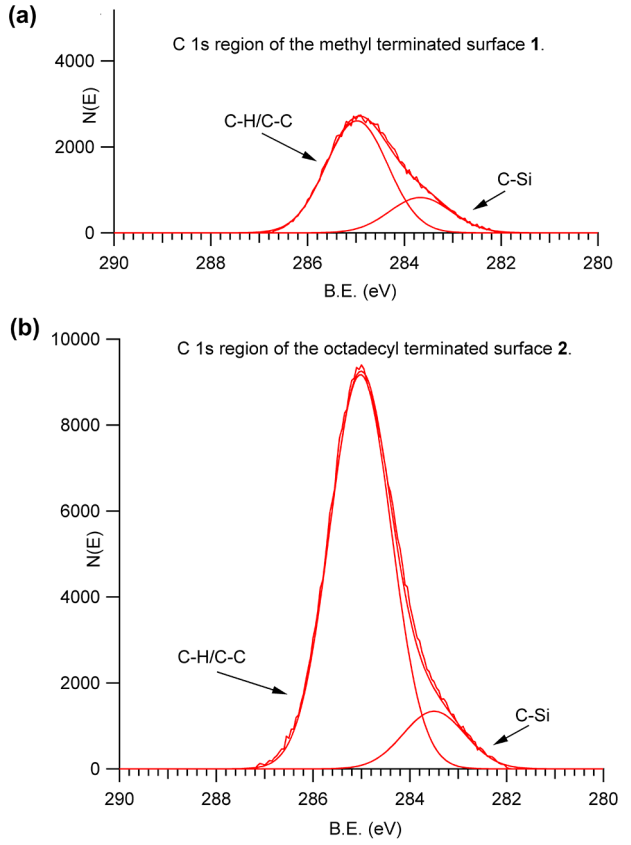

Figure 5. High-resolution XPS scans of the carbon 1s region of (a) surface **1** and (b) surface **2**.

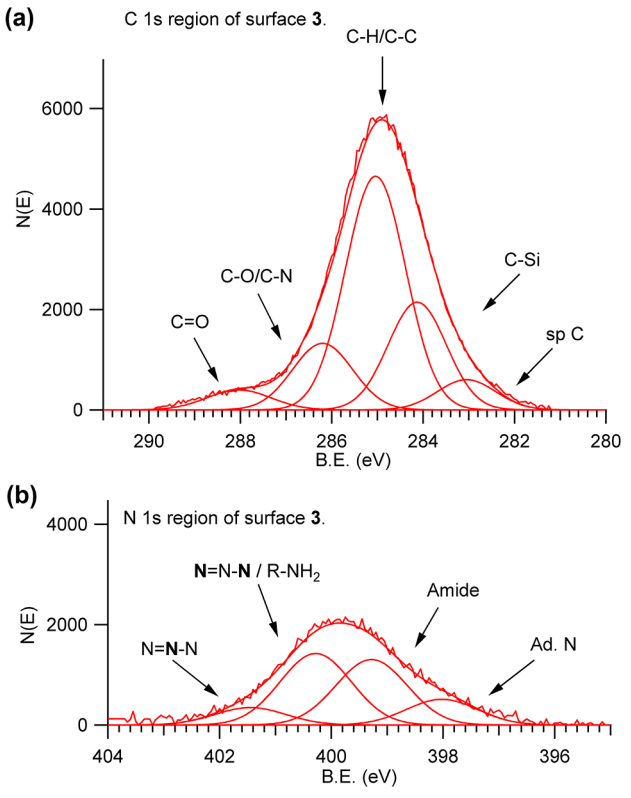

Figure 6. High-resolution XPS scan of (a) the carbon 1s region of surface **3** and (b) the nitrogen 1s region of surface **3**.

ally, the N=N–N/R–NH_2 peak centered at 400.3 eV (Figure 6b) has increased in magnitude relative to the C–NH_2 peak centered at 400.3 eV (Figure S1, Supporting Information) because of the additional nitrogen contribution from the 1s emission of the N1 (N–N=N) and N3 (N–N=N) of the triazole ring.[47,48] Both spectra were fit with peaks centered at 398.1 eV (Figure 6b, Ad. N peak) in agreement with the N 1s emission that is attributed to adventitious nitrogen and at 399.4 eV (Figure 6b, Amide peak) that is assigned to the amide nitrogen. The observed lower energy shift relative to 399.8 eV[43] is attributed to the amide nitrogen being in proximity to an electron donating group.

Further analysis of the N 1s region of surfaces **9** and **3** was used to quantitatively determine successful triazole formation; the calculations for this analysis are fully described in the Supporting Information. The results indicated that 31% of the propiolamides of **9** were successfully converted to the triazoles of **3** (Table 1). Overall, the XPS spectra in Figures 4–6 indicate

Table 1. Surface Reaction Yields Determined Using Quantitative Analysis of XPS

slide	dendronization (surface)	triazole formation (surface)
single layer		31% (**3**)
generation 1	36% (**4**)	31% (**6**)
generation 2	27% (**5**)	48% (**7**)

that XPS is a very useful method for the characterization of surfaces bearing alkyl, alkynyl, triazole-containing, and *β*-cyclodextrin functionalities. Based on comparison to these spectra and on additional in-depth analysis, XPS was used successfully to characterize and quantify the dendronized surfaces.

The XPS spectra of the C 1s and N 1s regions of dendronized surfaces **4** and **6** are shown in Figure 7. When the narrow C 1s spectra of **4** and **6** (Figure 7a,c) are compared to the C 1s spectrum of **3** (Figure 6a), important differences are notable. The C–O/C–N peaks for both **4** and **6** are larger than the same peak for **3** (288.1 eV), indicating the difference between the alkyl tether and the dendron. This peak arises from emissions of oxygen-bound carbons in the polyaryl ether dendrons and the nitrogen-bound carbons.[43,44] The C–O/C–N peak in Figure 7c for **6** is significantly larger than the same peak for **4** in Figure 7a, indicating that addition of *β*-cyclodextrin was successfully achieved. The O–C–O/C=O peak for **6** in Figure 7c is also larger than the C=O peak for **4** in Figure 7a, and this peak has a binding energy that is in agreement with the anomeric C 1s emission of the acetals present in 1,4-oligoglucosides. The size increase for this peak was attributed to the presence of the *β*-cyclodextrin present on the surface.[43,49,50] XPS C 1s spectra for **3**, **4**, and **6** (Figures 6a and 7a,c) all display a peak at 283.1 eV, indicating alkyne functionality is present. This is fully expected for compound **4** (Figure 7a) and indicates incomplete triazole formation (most likely because of steric hindrance) for **3** and **6**. Comparison of the spectra of the narrow scan N 1s regions for **3** (Figure 6b), **4** (Figure 7b), and **6** (Figure 7d) also indicates that the XPS spectra are as expected for the reported surfaces.[51,52]

Quantitative analysis of the N 1s region of surfaces **4** and **6** was used to quantify the percent dendronization of the terminal amines of surface **12** and the percent triazole formation to yield surface **6**. Equations are provided in the Supporting Information. Amine functionalized surface **12** was converted

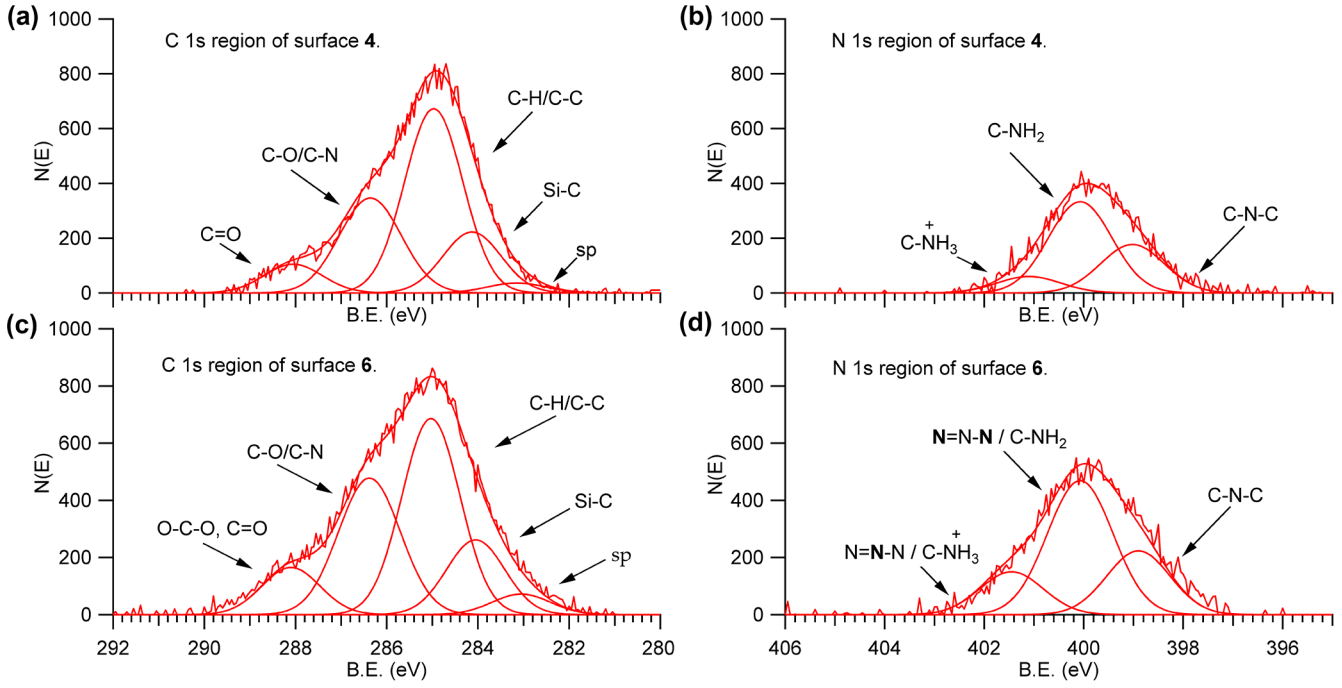

Figure 7. XPS spectra of G1 dendron functionalized surface **4** and β-cyclodextrin functionalized dendronized surface **6**. High-resolution scan of (a) the carbon 1s region of surface **4**, (b) the nitrogen 1s region of surface **4**, (c) the carbon 1s region of surface **6** and (d) the nitrogen 1s region of surface **6**.

to dendronized surface **4** with a 35% conversion rate. The same analysis was performed for the formation of G2 dendronized surface **5**, which was formed from **12** with 27% conversion. Addition of the bulkier G2 polyaryl system was less efficient. The percent triazole formation was calculated per dendron to be 31% and 48% for surfaces **6** (G1) and **7** (G2), respectively. Thus, the overall amounts of β-cyclodextrins on surfaces **6** and **7** was determined based on the combined yields for dendronization and triazole formation and was found to be very nearly equivalent. Because the overall amount of β-cyclodextrin on the dendronized surfaces was constant, the efficiency of binding of C152 to the dendronized surfaces is directly comparable (see below). The results garnered from the quantitative analysis of the XPS spectra of dendronized surfaces are summarized in Table 1.

Further characterization of the functionalized surfaces was performed using surface-specific VSFG spectroscopy. Figure 8 shows the *ssp* spectra of the β-cyclodextrin functionalized surface **3** (panel b), the first two generations of β-cyclodextrin functionalized dendrons **6** and **7** (panels c and d), and the methylated surface **1** for comparison purposes (Figure 8a).

Peak assignments for the methyl-terminated surface were described in the Experimental Methods. Assignments for the various β-cyclodextrin terminated surfaces have been made based on both previous experimental and computational Raman/IR data,[53] and previous SFG data.[40] All three β-cyclodextrin terminated surfaces share three main features at 2848, 2873, and 2943 cm^{-1}. The 2848 and 2943 cm^{-1} peaks have been assigned to the methylene symmetric and antisymmetric stretches, respectively. As these are well-documented frequencies for alkane methylene stretches, they are assigned to the alkane chain connecting the dendron—or simply the β-cyclodextrin—to the silica substrate. The assignment of the peak at 2873 cm^{-1} is less straightforward. This feature lies where one would expect a methyl symmetric

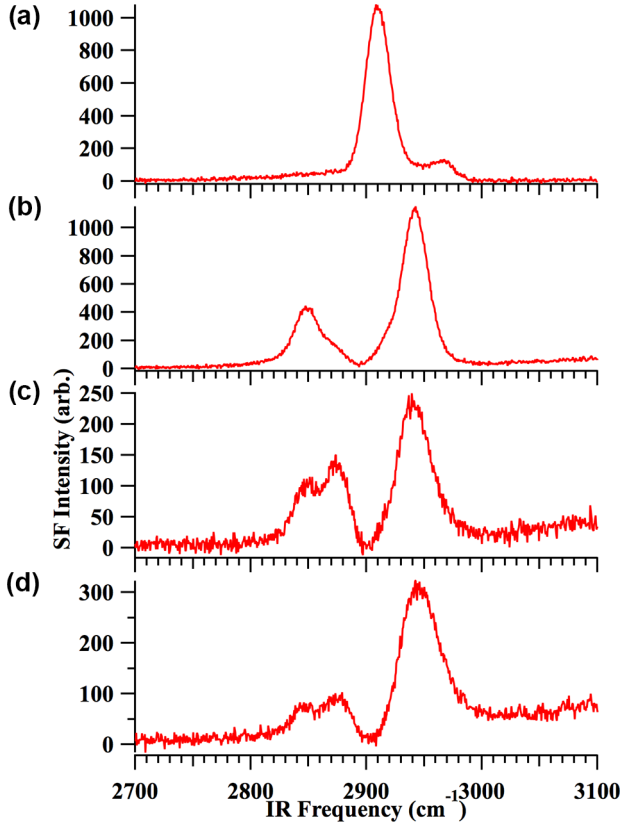

Figure 8. VSFG spectra of (a) methylated silica surface **1**, (b) a silica surface with tethered β-cyclodextrin **3**, (c) β-cyclodextrin functionalized generation 1 dendron surface **6**, (d) β-cyclodextrin functionalized generation 2 dendron surface **7**. All traces were taken in the *ssp* polarization combination.

dx.doi.org/10.1021/am504975y | ACS Appl. Mater. Interfaces 2014, 6, 18087−18097

stretch to occur, but no methyl groups are present on surfaces **6** or **7**. The most likely explanation for the peak at 2873 cm^{-1} is that it is due to the symmetric stretch of the methylene group directly adjacent to the silicon atom. As seen in Figure 8a, C−H stretches for the surface methyl groups that are directly adjacent to silicon atoms have been shown to shift to higher frequencies. One can also learn of general trends in orientational order by examining the signal/noise ratio. The peaks in the undendronized surface spectrum of **3** (Figure 8b) are distinctly more pronounced from the noise than the peaks in the spectra of either of the dendronized surfaces **6** or **7** (Figure 8c,d). The observed loss in signal/noise suggests that either fewer C−H containing functional groups are present on the surface or more orientational disorder occurs with the more bulky dendronized surfaces **6** and **7** than with **3**. The increased ability of the dendronized surfaces to bind C152 molecules (described below) provides evidence suggesting that the decrease in signal/noise is caused by a more disordered surface and not a less functionalized one.

To evaluate the ability of each surface to remove and retain solutes from aqueous solution, experiments were performed with a coumarin solute, C152, dissolved in aqueous solution. (Also, see Figure S3 in the Supporting Information.) In aqueous solution, C152's emission maximum is 527 nm, and the emission maximum is 424 nm in hexane. Upon the addition of *β*-cyclodextrin to the bulk aqueous solution, the maximum emission wavelength shifts 7 nm to a shorter wavelength, indicating that the *β*-cyclodextrin is binding to the C152 and changing the solute's local solvation environment.

The ability of *β*-cyclodextrin surfaces to retain C152 was tested using the procedure described in the Experimental Methods. The same general trends observed in the bulk solution measurements hold true for the surfaces. Figure 9 shows a blue-shift for C152 molecules both bound by *β*-cyclodextrin (503 nm) and adsorbed to the hydrophobic surface (499 nm) when compared to the unfunctionalized silica (511 nm). This observation matches the blue-shift seen upon addition of *β*-cyclodextrin to the bulk C152 solution and again suggests that adsorbed coumarins are experiencing a nonpolar environment. Functionalized surfaces showed repeatedly reproducible behavior with minimal signs of degradation after repeated cycling.

The sharp rise on the shorter wavelength ends of the spectra is due to scatter off the silica from the excitation light. This rise is present in both the functionalized and unfunctionalized slides and is extremely sensitive to slide position and angle. This scatter cannot be eliminated in a consistent manner from the individual spectra but contributes only minor inconsistencies in baselines and absolute emission intensities. Data in Figure 9 (red trace) shows that C152 adsorbs spontaneously to all three types of silica substrates—hydrophilic (panel a), hydrophobic (panel b), and *β*-cyclodextrin terminated (panel c)—but adsorbed C152 is retained only by the *β*-cyclodextrin functionalized slide after rinsing with water (dotted green and short dashed blue traces are comparable to black dashed traces in panels a and b but not in panel c). This observation reinforces the hypothesis that retention of the dye by cyclodextrin functionalized surfaces is due to specific binding interactions between *β*-cyclodextrin and C152, and that regardless the number of C152 molecules nonspecifically bound to hydrophobic interfaces, they are all removed upon rinsing with water. As noted in the Experimental Section, the fluorescence results are sensitive to slide positioning; the blue

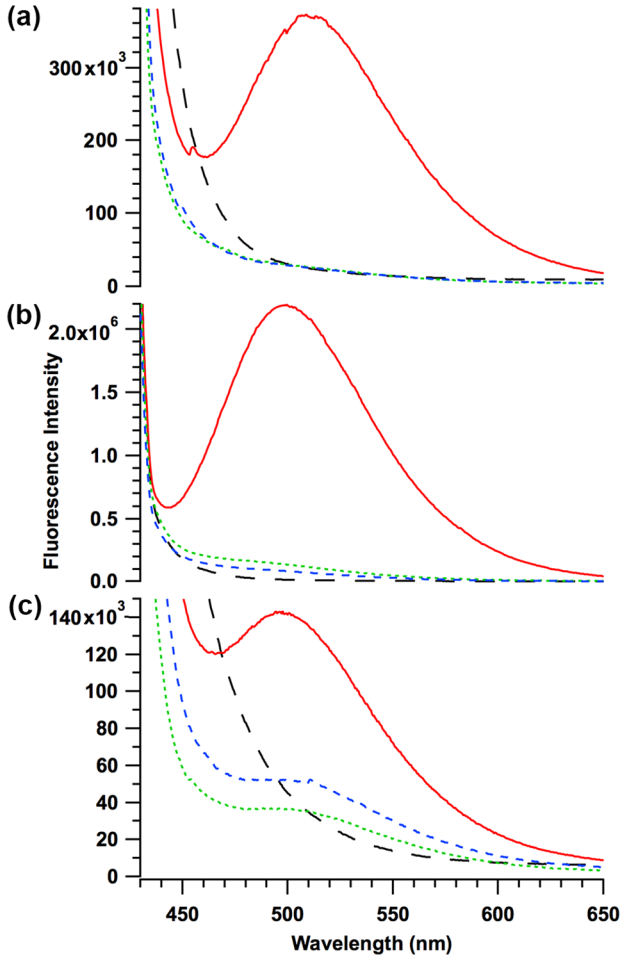

Figure 9. Coumarin 152 adsorbed to (a) a clean slide, (b) a methyl functionalized slide **1**, and (c) a *β*-cyclodextrin functionalized slide **3** (black) prior to addition of the solution, (red) after 1 h of equilibration in the solution, (green) after the first soak in water, and (blue) after the second soak in water.

and green traces in Figure 9 are equivalent within experimental limits.

Figure 10 shows that similar data is acquired from the slides functionalized with *β*-cyclodextrin bound to first- and second-generation dendrons **6** and **7**. Both samples appear to retain C152 following several 60 s rinses with pure water. Furthermore, the emission wavelength of the C152 bound by both generations of *β*-cyclodextrin dendrons (503 nm) is consistent with the wavelength of the C152 bound by surface **3** with *β*-cyclodextrin functionalization but lacking the dendron subcomponent. To summarize these results, only a short (60 s) washing time was required to remove nonspecifically bound C152 from **6** (G1); repeated washings of surface **6** do not reduce the amount of C152 that is bound. For surface **7** (G2), a second washing did remove additional C152, indicating that more C152 is bound nonspecifically to **7** and that **7** less effectively retains the solute from the solution via a specific binding mechanism.

While Figures 9 and 10 show that all of the slides functionalized with *β*-cyclodextrin retained C152, the fluorescence data from the silica surfaces cannot resolve the absolute amount of C152 retained. To quantify the relative capacities of the three different surfaces, each sample was rinsed with 50 mL of methanol to remove all detectable C152 from

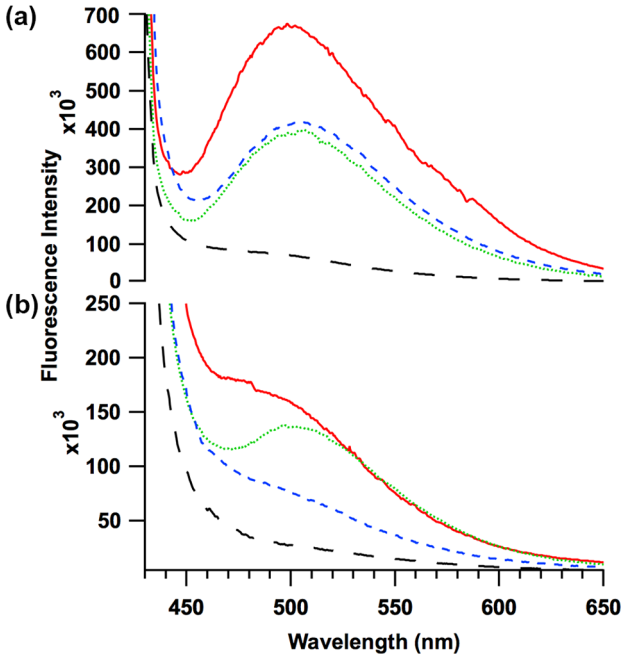

Figure 10. Coumarin 152 adsorbed to (a) β-cyclodextrin functionalized generation 1 dendron surface **6** and (b) β-cyclodextrin functionalized generation 2 dendron surface **7** (black) prior to introduction to the solution, (red) after 1 hour of equilibration in the solution, (green) after the first soak in water, and (blue) after the second soak in water.

the surface. Figure 11 shows retention of C152 after a 60 s wash in water and complete desorption triggered by sonication in methanol. The fluorescence excitation intensity of the wash was measured and compared to the excitation from prepared C152/methanol standards. The amount of C152 rinsed from each sample was assumed to represent the accessible number of β-cyclodextrin sites on the surface, and this number was

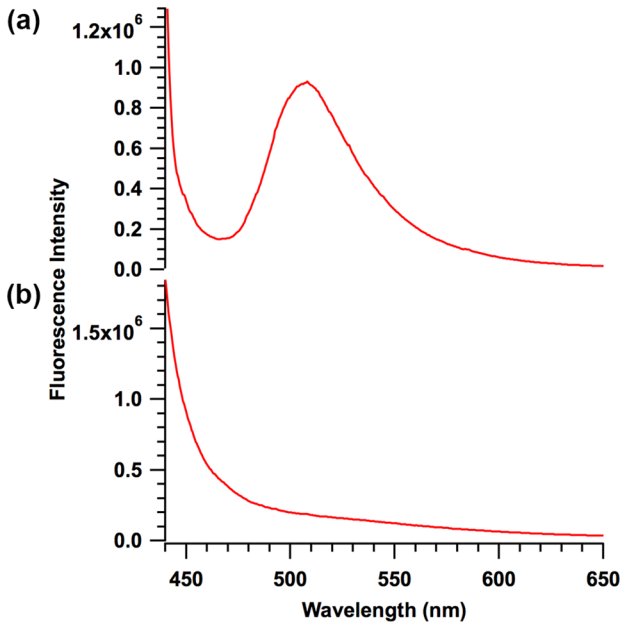

Figure 11. Representative spectra showing (a) retention of C152 after a 60 s wash in water and (b) complete desorption triggered by sonication in methanol.

converted into a surface coverage of β-cyclodextrins capable of forming complexes with organic solutes in aqueous solution. The spectra from the methanol washes of **6** and **7** are shown in Figure 12. With regard to Coumarin concentrations used in

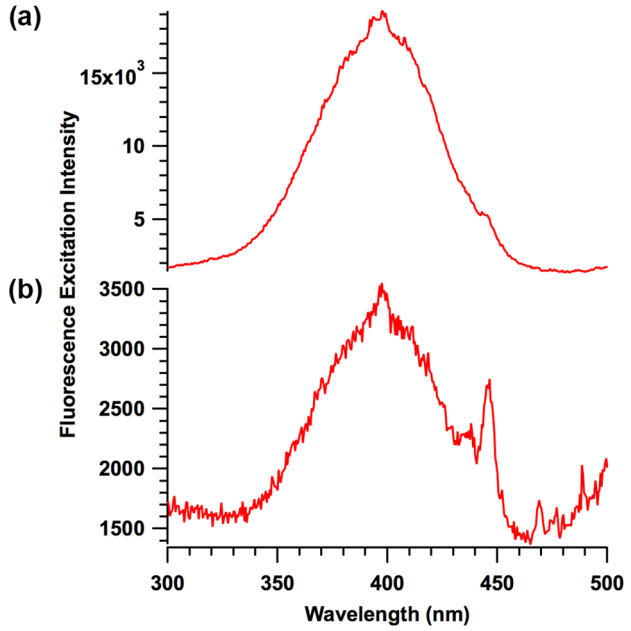

Figure 12. Representative spectra of the methanol wash from (a) surface **6** and (b) surface **7**.

these experiments (2.6 mg/L), these concentrations are higher than are typical for regulated pesticides in groundwater but only by a factor of ~3−4 in some cases. The signal-to-noise of our reported data exceeded 10 in many instances, inspiring confidence that these functionalized surface can, in fact, be relevant for wastewater remediation. The results, which are summarized in Table 2, were informative: silica surfaces

Table 2. Summary of Results for the Quantification of Desorbed C152

slide (compd)	[C152] (nM)	C152 molecules/cm^2 ($\times 10^{13}$)
single layer (**3**)	11	3
generation 1 (**6**)	78	20
generation 2 (**7**)	44	10

functionalized with first-generation dendrons **6** showed the highest C152 binding capacity with a surface coverage of 2×10^{14} sites/cm^2, followed by second-generation dendrons **7** with 1×10^{14} sites/cm^2 and finally β-cyclodextrin functionalized slides **3** with 3×10^{13} sites/cm^2. All values are the average of at least three trials.

As expected, both β-cyclodextrin dendronized surfaces **6** and **7** adsorb more analyte molecules than surface **3**, which presented singly tethered β-cyclodextrin molecules at the surface. The observation that the first-generation dendronized surface **6** adsorbs more C152 than the second-generation surface **7** is counterintuitive, however, because both surfaces bear the same overall amount of β-cyclodextrin. One likely explanation for the fact that surface **6** shows twice the binding capability of surface **7** is that many of the terminal β-cyclodextrin hosts on the second-generation dendron of **7** are inaccessible for binding by C152. The larger dendron appears

dx.doi.org/10.1021/am504975y | ACS Appl. Mater. Interfaces 2014, 6, 18087−18097

to angle more of its terminal cyclodextrins toward the surface so that they are unable to encapsulate C152 because of steric crowding of large β-cyclodextrins on the dendron. Although dendronization of **12** did not occur quantitatively en route to the formation of either **6** or **7**, the increased density of coumarin binding sites available for adsorption of C152 using dendronized surfaces still enabled the adsorption of more C152 than could be adsorbed on the nondendronized surface **3**.

CONCLUSIONS

Novel β-cyclodextrin functionalized silica surfaces that absorb targeted analytes from bulk aqueous solutions were synthesized and characterized. First- and second-generation polyaryl ether dendrons were tethered to silica surfaces. Cu(I) catalyzed cycloaddition "click" chemistry was used to append β-cyclodextrin onto the dendronized surfaces, and a β-cyclodextrin functionalized surface without the dendron was also reported for comparison purposes. These complex surfaces were characterized using XPS and VSFS analyses. Both techniques indicated that the proposed architecture was successfully synthesized. Although the synthesis procedure reported here was used for the appendage of β-cyclodextrin units onto dendronized surfaces, the route is highly flexible, and a wide variety of end groups can be added onto the alkynes on the dendrons via triazole formation. Different generations of dendrons afford different surface densities for the end group functionality.

These surfaces possess the adsorption and retention capabilities for which they were designed: the functionalized surfaces can be used repeatedly with highly reproducible results. The adsorption ability was observed from fluorescence spectra of the functionalized slides. These results showed that C152 had an affinity for the β-cyclodextrin functionalized surfaces that persisted through multiple aqueous washings. Additionally, the adsorptive capabilities of the slides were quantified by analyzing the wash from the slides after desorption was triggered. These results indicate that substrates functionalized with first-generation dendrons had a greater binding capacity than slides functionalized either with monomeric β-cyclodextrin or with larger generation dendrons. This result can be understood in terms of the trade-off between maximizing the density of β-cyclodextrin on the surface versus maximizing the number of β-cyclodextrins that can be accessed by a binding partner such as C152. The studies reported here have provided a methodology for characterizing and evaluating the properties of novel, highly functional surfaces.

ASSOCIATED CONTENT

Supporting Information

XPS of nitrogen 1S region of **9**; fluorescence spectra for an aqueous solution of C152 with and without CD, for C152 adsorbed to a CD functionalized surface, and for C152 in hexane; calibration plot for quantifying wash from functionalized slides; and the equations used for the quantitative XPS analysis of surface functionalization. This material is available free of charge via the Internet at http://pubs.acs.org.

AUTHOR INFORMATION

Corresponding Authors

*E-mail: mcloninger@chemistry.montana.edu
*E-mail: rawalker@chemistry.montana.edu.

Author Contributions

‡These authors contributed equally. The manuscript was written through contributions of all authors. All authors have given approval to the final version of the manuscript.

Notes

The authors declare no competing financial interest.

ACKNOWLEDGMENTS

This work was supported by NSF ICC 1026870.

REFERENCES

(1) United States Environmental Protection Agency. *Standards and Risk Management*. http://water.epa.gov/drink/standardsriskmanagement.cfm.
(2) Jain, A. K.; Gupta, V. K.; Jain, S. Suhas Removal of Chlorophenols Using Industrial Wastes. *Environ. Sci. Technol.* **2004**, *38*, 1195−1200.
(3) Johnson, A. C.; Sumpter, J. P. Removal of Endocrine-Disrupting Chemicals in Activated Sludge Treatment Works. *Environ. Sci. Technol.* **2001**, *35*, 4697−4703.
(4) Mifflin, A. L.; Konek, C. T.; Geiger, F. M. Tracking Oxytetracyline Mobility Across Environmental Interfaces by Second Harmonic Generation. *J. Phys. Chem. B* **2006**, *110*, 22577−22585.
(5) Azam, M. S.; Fenwick, S. L.; Gibbs-Davis, J. M. Orthogonally Reactive SAMs as a General Platform for Bifunctional Silica Surfaces. *Langmuir* **2011**, *27*, 741−750.
(6) Chen, E. H.; Walter, S. R.; Nguyen, S. T.; Geiger, F. M. Arylsilanated SiO_x Surfaces for Mild and Simple Two-Step Click Functionalization with Small Molecules and Oligonucleotides. *J. Phys. Chem. C* **2012**, *116*, 19886−19892.
(7) Diaz, J. A.; Grewer, D. M.; Gibbs-Davis, J. M. Tuning Ratios, Densities, and Supramolecular Spacing in Bifunctional DNA-Modified Gold Nanoparticles. *Small* **2012**, *8*, 873−883.
(8) Rekharsky, M. V.; Inoue, Y. Complexation Thermodynamics of Cyclodextrins. *Chem. Rev.* **1998**, *98*, 1875−1917.
(9) Schofield, W. C. E.; Bain, C. D.; Badyal, J. P. S. Cyclodextrin-Functionalized Hierarchical Porous Architectures for High-Throughput Capture and Release of Organic Pollutants from Wastewater. *Chem. Mater.* **2013**, *24*, 1645−1653.
(10) Schofield, W. C. E.; Badyal, J. P. S. Controlled Fragrant Molecule Release from Surface-Tethered Cyclodextrin Host-Guest Inclusion Complexes. *ACS Appl. Mater. Interfaces* **2011**, *3*, 2051−2056.
(11) Kellersberger, K. A.; Dejsupa, C.; Liang, Y. J.; Pope, R. M.; Dearden, D. V. Gas Phase Studies of Ammonium-Cyclodextrin Compounds Using Fourier Transform Ion Cyclotron Resonance. *Int. J. Mass Spectrom.* **1999**, *193*, 181−195.
(12) Szejtli, J. Introduction and General Overview of Cyclodextrin Chemistry. *Chem. Rev.* **1998**, *98*, 1743−1753.
(13) Nad, S.; Kumbhakar, M.; Pal, H. Photophysical Properties of Coumarin-152 and Coumarin-481 Dyes: Unusual Behavior in Nonpolar and in Higher Polarity Solvents. *J. Phys. Chem. A* **2003**, *107*, 4808−4816.
(14) Nad, S.; Pal, H. Unusual Photophysical Properties of Coumarin-151. *J. Phys. Chem. A* **2001**, *105*, 1097−1106.
(15) Roy, D.; Piontek, S.; Walker, R. A. Surface Induced Changes in Coumarin Solvation and Photochemistry at Polar Solid/Liquid Interfaces. *Phys. Chem. Chem. Phys.* **2011**, *13*, 14758−14766.
(16) Ooshika, Y. Absorption Spectra of Dyes in Solution. *J. Phys. Soc. Jpn.* **1954**, *9*, 594−602.
(17) McRae, E. G. Theory of Solvent Effects on Molecular Electronic Spectra. Frequency Shifts. *J. Phys. Chem.* **1957**, *61*, 562−572.
(18) Reynolds, L.; Gardecki, J. A.; Frankland, S. J. V.; Horng, M. L.; Maroncelli, M. Dipole Solvation in Nondipolar Solvents: Experimental Studies of Reorganization Energies and Solvation Dynamics. *J. Phys. Chem.* **1996**, *100*, 10337−10354.
(19) Jones, G.; Jackson, W. R.; Kanoktanaporn, S.; Halpern, A. M. Solvent Effects on Photophysical Parameters for Coumarin Laser-Dyes. *Opt. Commun.* **1980**, *33*, 315−320.

(20) Horng, M. L.; Gardecki, J. A.; Papazyan, A.; Maroncelli, M. Subpicosecond Measurements of Polar Solvation Dynamics: Coumarin-153 Revisited. *J. Phys. Chem.* **1995**, *99*, 17311−17337.
(21) Gardecki, J. A.; Maroncelli, M. Comparison of the Single-Wavelength and Spectral-Reconstruction Methods for Determining the Solvation-Response Function. *J. Phys. Chem. A* **1999**, *103*, 1187−1197.
(22) Jones, R. L.; Pearsall, N. C.; Batteas, J. D. Disorder in Alkylsilane Monolayers Assembled on Surfaces with Nanoscopic Curvature. *J. Phys. Chem. C* **2009**, *113*, 4507−4514.
(23) Byun, H.-S.; Zhong, N.; Bittman, R. 6^{A}-O-p-Toluenesulfonyl-β-Cyclodextrin. *Org. Synth.* **2004**, *10*, 690.
(24) Petter, R. C.; Salek, J. S.; Sikorski, C. T.; Kumaravel, G.; Lin, F. T. Cooperative Binding by Aggregated Mono-6-(alkylamino)-beta-cyclodextrins. *J. Am. Chem. Soc.* **1990**, *112*, 3860−3868.
(25) Ortega-Munoz, M.; Lopez-Jaramillo, J.; Hernandez-Mateo, F.; Santoyo-Gonzalez, F. Synthesis of Glyco-Silicas by Cu(I)-Catalyzed "Click-Chemistry" and Their Applications in Affinity Chromatography. *Adv. Syn. Catal.* **2006**, *348*, 2410−2420.
(26) Wang, Y.; Xiao, Y.; Tan, T. T. Y.; Ng, S.-C. Click Chemistry for Facile Immobilization of Cyclodextrin Derivatives onto Silica As Chiral Stationary Phases. *Tetrahedron Lett.* **2008**, *49*, 5190−5191.
(27) Antoni, P.; Nystrom, D.; Hawker, C. J.; Hult, A.; Malkoch, M. A Chemoselective Approach for the Accelerated Synthesis of Well-Defined Dendritic Architectures. *Chem. Commun.* **2007**, 2249−2251.
(28) Malkoch, M.; Schleicher, K.; Drockenmuller, E.; Hawker, C. J.; Russell, T. P.; Wu, P.; Fokin, V. V. Structurally Diverse Dendritic Libraries: A Highly Efficient Functionalization Approach Using Click Chemistry. *Macromolecules* **2005**, *38*, 3663−3678.
(29) Hawker, C. J.; Frechet, J. M. J. Preparation of Polymers with Controlled Molecular Architecture. A New Convergent Approach to Dendritic Macromolecules. *J. Am. Chem. Soc.* **1990**, *112*, 7638−7647.
(30) Choma, J.; Dziura, A.; Jamiola, D.; Nyga, P.; Jaroniec, M. Preparation and Properties of Silica-Gold Core-Shell Particles. *Colloids Surf., A* **2011**, *373*, 167−171.
(31) Iliashevsky, O.; Amir, L.; Glaser, R.; Marks, R. S.; Lemcoff, N. G. Synthesis, Characterization, And Protein Binding Properties of Supported Dendrons. *J. Mater. Chem.* **2009**, *19*, 6616−6622.
(32) Walton, J.; Wincott, P.; Fairley, N.; Carrick, A. *Peak Fitting with CasaXPS*.; Accolyte Science: Knutsford, U.K., 2010.
(33) D'Acunzi, M.; Mammen, L.; Singh, M.; Deng, X.; Roth, M.; Auernhammer, G. K.; Butt, H.-J.; Vollmer, D. Superhydrophobic Surfaces by Hybrid Raspberry-Like Particles. *Faraday Discuss.* **2010**, *146*, 35−48.
(34) Li, Z. B.; Rutan, S. C. Solvatochromic Studies of the Surface Polarity of Silica Under Normal-Phase Conditions. *Anal. Chim. Acta* **1995**, *312*, 127−139.
(35) Richmond, G. L. Molecular Bonding and Interactions at Aqueous Surfaces As Probed by Vibrational Sum Frequency Spectroscopy. *Chem. Rev.* **2002**, *102*, 2693−2724.
(36) Bain, C. D. Sum-Frequency Vibrational Spectroscopy of the Solid-Liquid Interface. *J. Chem. Soc., Faraday Trans.* **1995**, *91*, 1281−1296.
(37) Lambert, A. G.; Davies, P. B.; Neivandt, D. J. Implementing the Theory of Sum Frequency Generation Vibrational Spectroscopy: A Tutorial Review. *Appl. Spectrosc. Rev.* **2005**, *40*, 103−145.
(38) Gobrogge, E. A.; Woods, B. L.; Walker, R. A. Liquid Organization and Solvation Properties at Polar Solid/Liquid Interfaces. *Faraday Discuss.* **2013**, *167*, 309−327.
(39) Ding, F.; Zhong, Q.; Brindza, M. R.; Fourkas, J. T.; Walker, R. A. Ti:Sapphire, Broadband Vibrational Sum-Frequency Generation Spectrometer with a Counter-Propagating Geometry. *Opt. Express* **2009**, *17*, 14665−14675.
(40) Li, X. Q.; Messmer, M. C. Comparison of Model Monomeric and Polymeric Alkyl Stationary Phases on Silica Using Sum-Frequency Spectroscopy. *J. Chromatogr. A* **2003**, *984*, 19−28.
(41) Huisgen, R.; Bayer, H. O.; Schaefer, F. C.; Gotthardt, H. New Type of Mesoionic Aromatic Compound and its 1,3-Dipolar Cycloaddition Reactions with Acetylene Derivatives. *Angew. Chem., Int. Ed.* **1964**, *3*, 136−137.
(42) Rostovtsev, V. V.; Green, L. G.; Fokin, V. V.; Sharpless, K. B. a Stepwise Huisgen Cycloaddition Process: Copper(I)-Catalyzed Regioselective "Ligation" Of Azides and Terminal Alkynes. *Angew. Chem., Int. Ed.* **2002**, *41*, 2596−2599.
(43) Beamson, G.; Briggs, D. *High Resolution XPS of Organic Polymers: The Scienta ESCA 300 Database*. John Wiley & Sons: Chichester, U.K., 1992.
(44) Ciampi, S.; Boecking, T.; Kilian, K. A.; James, M.; Harper, J. B.; Gooding, J. J. Functionalization of Acetylene-Terminated Monolayers on Si(100) Surfaces: A Click Chemistry Approach. *Langmuir* **2007**, *23*, 9320−9329.
(45) Liu, X.; Zheng, H.-N.; Ma, Y.-Z.; Yan, Q.; Xiao, S.-J. Microwave Irradiated Click Reactions on Silicon Surfaces via Derivertization of Covalently Grafted Poly(PEGMA) Brushes. *J. Colloid Interface Sci.* **2011**, *358*, 116−122.
(46) Neubauer, R.; Whelan, C. M.; Denecke, R.; Steinruck, H. P. the Thermal Chemistry of Saturated Layers of Acetylene and Ethylene on Ni(100) Studied by in Situ Synchrotron X-ray Photoelectron Spectroscopy. *J. Chem. Phys.* **2003**, *119*, 1710−1718.
(47) Liu, X.; Zheng, H.-N.; Ma, Y.-Z.; Yan, Q.; Xiao, S.-J. Microwave Irradiated Click Reactions on Silicon Surfaces via Derivertization of Covalently Grafted Poly(PEGMA) Brushes. *J. Colloid Interface Sci.* **2011**, *358*, 116−122.
(48) Daugaard, A. E.; Hvilsted, S.; Hansen, T. S.; Larsen, N. B. Conductive Polymer Functionalization by Click Chemistry. *Macromolecules* **2008**, *41*, 4321−4327.
(49) Freire, C. S. R.; Silvestre, A. J. D.; Neto, C. P.; Gandini, A.; Fardim, P.; Holmbom, B. Surface Characterization by XPS, Contact Angle Measurements, and ToF-SIMS of Cellulose Fibers Partially Esterified with Fatty Acids. *J. Colloid Interface Sci.* **2006**, *301*, 205−209.
(50) Belgacem, M. N.; Czeremuszkin, G.; Sapieha, S.; Gandini, A. Surface Characterization of Cellulose Fibres by XPS and Inverse Gas Chromatography. *Cellulose* **1995**, *2*, 145−157.
(51) Moses, P. R.; Wier, L. M.; Lennox, J. C.; Finklea, H. O.; Lenhard, J. R.; Murray, R. W. Chemically Modified Electrodes 0.9. X-Ray Photoelectron-Spectroscopy of Alkylamine-Silanes Bound to Metal-Oxide Electrodes. *Anal. Chem.* **1978**, *50*, 576−585.
(52) Hooper, A. E.; Werho, D.; Hopson, T.; Palmer, O. Evaluation of Amine- and Amide-Terminated Self-Assembled Monolayers as "Molecular Glues" For Au and SiO_2 Substrates. *Surf. Interface Anal.* **2001**, *31*, 809−814.
(53) Li, W.; Lu, B.; Sheng, A.; Yang, F.; Wang, Z. Spectroscopic and Theoretical Study on Inclusion Complexation of Beta-Cyclodextrin with Permethrin. *J. Mol. Struct.* **2010**, *981*, 194−203.